Supplementary Materials for:

Replication stress response defects are associated with response to immune checkpoint blockade in non-hypermutated cancers

Daniel J. McGrail[1*], Patrick G. Pilié[2], Hui Dai[1], Truong Nguyen Anh Lam[2], Yulong Liang[1], Leonie Voorwerk[3], Marleen Kok[3,4], Xiang H.-F. Zhang[5,6,7,8], Jeffrey M. Rosen[5,6], Amy B. Heimberger[9,10], Christine B. Peterson[11], Eric Jonasch[2] & Shiaw-Yih Lin[1*]

[1]Department of Systems Biology, The University of Texas MD Anderson Cancer Center, Houston, Texas 77030, USA.

[2]Department of Genitourinary Medical Oncology, The University of Texas MD Anderson Cancer Center, Houston, Texas 77030, USA.

[3]Division of Tumor Biology & Immunology, The Netherlands Cancer Institute, Amsterdam, the Netherlands.

[4]Department of Medical Oncology, The Netherlands Cancer Institute, Amsterdam, the Netherlands.

[5]Department of Molecular and Cellular Biology, Baylor College of Medicine, Houston, Texas 77030, USA.

[6]Dan L. Duncan Cancer Center, Baylor College of Medicine, Houston, Texas 77030, USA.

[7]Lester and Sue Smith Breast Center, Baylor College of Medicine, Houston, Texas 77030, USA.

[8]McNair Medical Institute, Baylor College of Medicine, Houston, Texas 77030, USA.

[9]Department of Neurological Surgery, Feinberg School of Medicine, Northwestern University, Chicago, Illinois 60611, USA.

[10]Malnati Brain Tumor Institute of the Lurie Comprehensive Cancer Center, Feinberg School of Medicine, Northwestern University, Chicago, Illinois 60611, USA.

[11]Department of Biostatistics, The University of Texas MD Anderson Cancer Center, Houston, Texas 77030, USA.

*Corresponding author. Email: djmcgrail@mdanderson.org or sylin@mdanderson.org

Materials and Methods

Cell lines, organoids, and syngeneic mammary tumor transplants

Table S1 contains detailed information of the source and culturing conditions for each cell line used in the study. In brief, cells were cultured at 37°C in humidified 95% air/5% CO_2. Cell lines were purchased from ATCC, DSMZ, CH3 Biosystems, or The University of Texas MD Anderson Cancer Center's Characterized Cell Line Core. Patient-derived xenografts were acquired from the Huntsman Cancer Institute University of Utah Preclinical Research Resource. STR profiling and routine mycoplasma testing were performed at The University of Texas MD Anderson Cancer Center's Characterized Cell Line Core.

Murine transplant models T11 and 2208L were derived from p53-null BALB/c mice. For in vitro studies with T11 and 2208L, cell lines were derived by digesting minced tumors in 400 U/mL collagenase IV and 100 U/mL hyaluronidase before culturing in RPMI1640 supplemented with 10% FBS, 1% penicillin-streptomycin, and 1.25 μg/mL amphotericin B.

For organoid models, breast cancer patient-derived xenografts were expanded in athymic nu/nu mice as previously described *(58, 60)*. Once tumors reached ~500 mm^3 they were resected to generate organoids. Tumors were finely minced and then digested for 1 to 2 hours at 37°C with agitation using 1.5 mg/mL collagenase (Sigma-Aldrich, C9407) diluted in organoid growth media (Invitrogen Advanced DMEM/F12 supplemented with 5% FBS, 5 ng/mL EGF, 1x B27, 5 μM Y-27632, 500 nM A83-01, 500 nM SB202190, 1.25 mM N- acetylcysteine, 5 mM nicotinamide, 10 mM HEPES, 2 mM glutamine, 50 μg/mL Primocin, 100 U/mL penicillin, and 100 μg/mL streptomycin) *(61)*. Undigested tumor fragments were removed by straining through a 100 μm filter before pelleting cells by centrifugation. RBCs were lysed using RBC lysis buffer

(BioLegend) as necessary. Isolated cells were re-suspended in ice-cold Cultrex growth factor-reduced Basement Membrane Extract (BME) type 2 (Trevigen), and 50 µL drops were applied to pre-warmed 24-well plates. After allowing BME to polymerize for 1 hour at 37°C, organoid growth media was added to each well. Organoids were passaged by digestion with TrypLE Express. All experiments were performed with organoids below passage 3.

Animals

Mice aged 6 to 8 weeks were used for all studies. Female mice were used for all breast cancer studies. Male mice were used for all renal cell carcinoma studies, as RAG cells failed to robustly grow in female mice. BALB/c, C57BL/6, FVB, and immunodeficient NCG (NOD-*Prkdc*^{em26Cd52}*Il2rg*^{em26Cd22}/NjuCrl) mice were all acquired from Charles River. Before treatment initiation, mice were blindly randomized to ensure equal starting volume for all treatment groups. If mice required euthanasia for tumor ulceration in absence of excessive tumor burden those mice were censored at the day requiring euthanasia and are indicated by hashes on the plots. Animal numbers were determined from previous literature with no additional statistical methods used to determine sample size. Blinded investigators performed tumor measurements. All experiments involving animals were approved by the Institutional Animal Care and Use Committee.

Replication stress response defect (RSRD) score

The RSRD signature *(25)* was used to determine RSRD score by multiplying the signature coefficient of each gene by the z-normalized expression value, and then dividing the value by the sum of the absolute values of the signature coefficients. Gene expression for cell lines was acquired from the CCLE *(62)*.

RSR defect cell cycle assay

The ability of cells to recover from replication stress was performed as previously described*(25, 63–66)*. Replication stress was induced by treatment with 2 mM hydroxyurea (HU) for 16 hours to deplete nucleotides. Control cells were mock-treated with water. Cells were then either harvested (t = 0 hours) or washed and released into pre-equilibrated media containing 1 μg/mL nocodazole for 10 hours to collect cells in G2/M phase. For organoid experiments, cells were released for 24 hours instead of 10 hours. For roscovitine experiments, cells were pretreated for 2 hours with 10 μM roscovitine (Selleck) or DMSO vehicle control. Cells were fixed with ice-cold 70% ethanol. DNA was stained with 20 μg/mL propidium iodide (Calbiochem) in PBS containing 400 μg/mL RNase A (Invitrogen) for 20 minutes before analysis by flow cytometry. Data were processed using FlowJo.

DNA fiber analysis

For analysis of replication fork restart, cells were labeled with 25 μM CldU for 20 minutes before treatment with 2 mM HU for 2 hours. Cells were washed with growth media, which had been equilibrated overnight in a cell culture incubator and moved to 25 μM IdU for 45 minutes before harvesting. For roscovitine experiments, cells were pretreated for 2 hours with 10 μM roscovitine or DMSO vehicle control. Cell were collected by trypsinization, washed in ice-cold PBS, and lysed in spreading buffer (200 mM Tris-HCl pH 8.0, 50 mM EDTA, 0.5% SDS). Drops (5 μL) of lysate were pipetted onto microscope slides and allowed to run slowly down the slide. Slides were air-dried, fixed in methanol/acetic acid (3:1) for 10 min, washed with water, and allowed to dry. For staining, DNA was denatured in 2N HCl for 30 minutes, washed in PBS, and blocked with 5% normal horse serum in PBS for 1 hour. Primary antibodies against CldU (rat anti-BrdU, clone BU1/75 (ICR1), Abcam, 1:600 dilution) and IdU (mouse anti-BrdU, clone B44, BD Biosceinces, 1:300 dilution) were diluted in blocking buffer and incubated overnight at 4°C. The slides were

washed with high salt TBS-T (1M NaCl, 0.5% Tween 20, 50 mM Tris-HCl, pH 8.0) followed by PBS and fixed in 2% paraformaldehyde. After rinsing, the slides were incubated with anti-Rat AlexaFluor 488 antibody (1:500) and anti-Mouse AlexaFluor 568 antibody (1:500) diluted in blocking buffer for 1 hour at room temperature. After washing, the slides were mounted in Vectashield and imaged using a Nikon Eclipse TE100. Percentage of failed replication forks is defined as the number dual-labeled fibers divided by the total number of green CldU fibers. For analysis of replication fork speed, we used the conversion factor of 2.59 kb/μm*(67)*.

Immunofluorescence for nuclear DNA damage markers

Soluble proteins were extracted with cytoskeletal buffer (10 mM PIPES pH 6.8, 100 mM NaCl, 300 mM sucrose, 3mM MgCl2, 1mM EGTA, 0.5% Triton-X100) before formaldehyde fixation. Fixed cells were permeabilized with 1% Triton-X100, blocked in 5% horse serum, and then stained with desired antibodies at room temperature for 1 hour diluted in blocking buffer (table S2). For staining phosphorylated ATM/ATR substrates with anti-pSQ/TQ*(59)*, cells were also extracted with stripping buffer (10 mM Tris-HCl pH 7.4, 10 mM NaCl, 3mM $MgCl^2$, 1% Tween 40, 0.25% sodium deoxycholate) before fixation. For staining single-strand DNA breaks by native CldU*(68)*, cells were cultured in 25 μM CldU for 2 days before staining. For EdU, cells were treated with 10 μM EdU 30 minutes prior to HU treatment or 30 minutes prior to fixation for control cells. Biotin was conjugated to EdU by 15-minute incubation in CLICK reaction buffer (10 mM HEPES, 10 mM sodium ascorbate, 10 μM azide-PEG3-biotin, and 2 mM $CuSO_4$ in PBS), which was visualized using streptavidin secondary antibodies. For roscovitine experiments, cells were pretreated for 2 hours with 10 μM roscovitine or DMSO vehicle control. Imaging was performed on a Nikon Eclipse TE2000E, capturing all images for a given replicate simultaneously to assure no variances in light intensity. All image analysis was performed in MATLAB (MathWorks). For

quantification, foci and nuclei were segmented, and then the integrated intensity of all foci normalized to cell area was taken as staining intensity.

Analysis of RPA exhaustion

Cells were either HU (2 mM) or mock-treated for 6 hours before staining for RPA and ssDNA by native CldU as described above. Nuclei were segmented, and DNA (DAPI) intensity was used to identify actively cycling cells. The median ssDNA/RPA intensity of cells in G0/G1 was used to normalize signal in actively cycling cells. Using non-transformed MCF-10A mammary epithelial cells, a regression line was fit on log-transformed RPA and ssDNA intensities, and an upper bound that encompassed 99.9% of MCF-10A cells was determined as a threshold for RPA exhaustion (see fig. S2C).

UV-resistant DNA synthesis assay

Cells were labeled with 10 μM BrdU for 30 minutes and then either UV-irradiated at 5 J/m^2 or mock-treated. Cells were moved to fresh growth media that had been equilibrated overnight in a cell culture incubator, then incubated for 30 minutes before adding 10 μM EdU for another 30 minutes. Cells were fixed with formaldehyde, and DNA was denatured with 2N HCl and permeabilized with 1% Triton-X100 before CLICK reaction as described above. After blocking in 5% horse serum, BrdU was stained using the mouse anti-BrdU clone B44. Anti-mouse AlexaFluor 488 and Streptavidin 596 were used for detection. For quantification, individual nuclei were segmented by DAPI and used to determine the integrated intensity of BrdU and EdU. The intensity of EdU (post-UV DNA synthesis) was determined in BrdU-positive cells, and then the median value in UV-treated cells was normalized to mock-treated cells to determine relative inhibition of DNA synthesis.

Cytosolic ssDNA immunofluorescence

Cytosolic ssDNA was stained essentially as described *(69, 70)*. Formalin-fixed cells were selectively permeabilized with 0.5% saponin and blocked with 5% normal horse serum. Mouse anti-ssDNA (Millipore Sigma MAB3868) was incubated overnight (50 μg/mL in blocking buffer) at 4°C. The following day, cells were washed and incubated with anti-Mouse AlexaFluor 488 antibody (1:500) diluted in blocking buffer for 1 hour at room temperature. Coverslips were sealed using VectaShield with DAPI. Imaging was performed on a Nikon Eclipse TE2000E. For quantification, ssDNA intensity was normalized to the number of cells in each image determined by DAPI nuclear counterstain.

Quantification and visualization of cytosolic DNA by cell fractionation

Cells were harvested by trypsinization, washed in ice-cold PBS, and resuspended in ice-cold hypotonic lysis buffer (20 mM HEPES pH 7.4, 10 mM KCl, 2 mM $MgCl_2$, 1 mM EDTA, and 1 mM EGTA, with 1 mM DTT and 1x protease inhibitors added immediately before use). After 15 minute incubation on ice, cells were sheared through a 27g needle and incubated for an additional 15 minutes on ice. Nuclei were pelleted by brief centrifugation at 2,000 rcf, and remaining mitochondria and other debris were cleared by centrifugation at 15,000 rcf for 15 minutes. Cytosolic DNA was quantified using a Qubit 4 with the Qubit HS dsDNA and Qubit ssDNA assay kits. For quantification of ssDNA, lysates were digested with 20 μg/mL RNase A prior to analysis. As the ssDNA kit can detect both ssDNA and dsDNA, the dsDNA concentration was subtracted from the ssDNA concentration for analysis. Cytosolic DNA concentrations were normalized to cytosolic protein as determined by BCA assay. To analyze size of cytosolic DNA by electrophoresis, cytosolic extracts were subject to proteinase K digestion followed by precipitation with 10 mM $MgCl_2$, 0.5M ammonium acetate, and 67% ethanol. Cytosolic DNA precipitates were

washed in 70% ethanol before, re-solubilized in TE buffer, and then analyzed by BioAnalyzer. In some experiments, DNA precipitates were treated with ssDNA-specific S1 nuclease (Thermo Fisher Scientific) or dsDNA-specific dsDNase (Thermo Fisher Scientific product #EN0771) per manufacturer's instructions.

Western blotting

Cells were lysed in urea buffer (8 M urea, 150 mM β-mercaptoethanol, and 50 mM Tris/HCl, pH 7.5) by sonication, and cleared by centrifugation. Protein concentration was determined by Bradford (Bio-Rad) quantification kit. Proteins were separated by gel electrophoresis transferred to nitrocellulose (Bio-Rad) membranes, and then probed with desired antibodies (see Table S2).

siRNA and shRNA experiments

Mission siRNAs were acquired from Sigma-Aldrich, and transfected into cells using Lipofectamine 3000 (Invitrogen) per manufacturer's instructions. Cells were incubated for 2 days prior to performing desired experiments. For generation of stable cell lines expressing with shRNA, cells were transduced with Dharmacon GIPZ lentiviral constructs in the presence of 8 μg/mL polybrene before selection of stable cell lines with puromycin. Catalogue numbers for all siRNAs and shRNAs utilized are given in table S3.

RNA-seq of murine renal models

RNA was extracted from RENCA and RAG cells using a QIAGEN RNeasy kit, with 3 independent biological replicates per cell line. After confirming RNA purity by spectroscopy and integrity by BioAnalyzer, RNA sequencing was performed by NovoGene. Raw FASTQ files were quantified to generate transcripts per million (TPM) using kallisto *(71)* (v0.44.0). Raw data are available in table S4.

In vivo studies

Mammary breast cancer cells were implanted into the mammary fat pad of female mice at the following cell numbers: $5x10^5$ E0771, $5x10^4$ T11, $5x10^5$ HRM-1, $5x10^4$ 4T1, or $2x10^6$ 2208L. Renal cancer cell lines RENCA ($5x10^5$ cells) and RAG ($1x10^7$ cells) were implanted into male mice, as RAG cells did not form tumors in female mice. All tumors were grown ~150 mm^3 before treatment initiation, roughly 10-20 days post-implantation, as measured by calipers using the equation $V = L \times W^2 / 2$. Treatments were administered for a maximum of 1 month, after which any remaining mice were continually monitored for long-term survival. For immune checkpoint blockade (ICB) in breast cancer tumor models, mice were intraperitoneally injected thrice weekly (days 1/3/5) with 200 μg anti-PD1 (rat IgG2a, clone RMP1-14) and 100 μg anti-CTLA4 (hamster IgG, clone 9H10), or isotype controls (rat IgG2a Clone 2A3, polyclonal hamster IgG catalog #BE0087), all from BioXcell. For immune checkpoint blockade (ICB) in renal cancer tumor models, mice were intraperitoneally injected thrice weekly (days 1/3/5) with 200 μg anti-PD1 (rat IgG2a, clone RMP1-14) or isotype controls (rat IgG2a Clone 2A3). For prexasertib CHK1i combination therapy, 10 mg/kg of free prexasertib (12 mg/kg accounting for weight of salt), prexasertib/LY2606368 (Selleck), or vehicle control (20% captisol, Selleck) was injected subcutaneously BID (2208L) or QD (RENCA) on days 1 and 4, with ICB administered on days 2/4/6 as described above. For AZD7762 CHKi combination therapy, mice implanted with RSRD-low/ICB-resistant 4T1 cells were treated with 25 mg/kg AZD7762 (Selleck) or vehicle control (20% captisol) by intraperitoneal injection on days 1 and 2, with ICB administered per above on days 2/4/6. For roscovitine studies, mice were pretreated with 50 mg/kg roscovitine (Selleck) or vehicle control (20% captisol) by intraperitoneal injection for 3 days before initiating treatment with ICB. Thereafter, ICB was administered as above with continued daily roscovitine treatment.

Multispectral tissue staining

Slides were stained using Opal 4-color IHC Kit (NEL794001KT) from Perkin Elmer along with primary antibodies from Cell Signaling Technology for CD3 (clone D4V8L), CD4 (clone D7D2Z), FoxP3 (clone D6O8R), CD8 (clone D4W2Z), CD11c (clone D1V9Y), F4/80 (clone D2S9R), and CD31 (clone D8V9E). Formalin-fixed paraffin embedded tissues were sectioned, deparaffinized in xylene, and rehydrated through an ethanol gradient. Microwave treatment was applied to perform antigen retrieval, quench endogenous peroxidases, and remove antibodies from earlier staining procedures. Perkin Elmer AR6 Antigen retrieval buffer (pH 6) was used for all antibodies. The slides were scanned with the VECTRA image scanning system (Caliper Life Sciences), and signals were unmixed into a composite image with Vectra inForm software. For each tumor model, 5 independent tumors were imaged with at least 10 images per slide from arbitrary fields of view. Images showing appreciable necrosis were not used for analysis. Final quantification was performed using custom MATLAB scripts.

Patient cohorts treated with immune checkpoint blockade and analysis

For all patient cohorts, sample size was determined based on availability of data with no pre-defined power calculation. Further study information is found within the respective citations.

Metastatic breast cancer:

The TONIC breast cancer trial *(11)* data was acquired from EGAS0001003535, with associated patient outcome data and IHC data for TILs and PD-L1 expression on immune cells. Patients with stable disease of at least 24 weeks were or a CR/PR were considered responders, as well as one patient in the cyclophosphamide induction treatment arm, who had non-measurable disease according to RECIST1.1 but had clinical benefit for at least 24 weeks and was therefore regarded

as a responder. RNA-seq FASTQ files were quantified to generate transcripts per million (TPM) using kallisto *(71)* (v0.44.0).

Metastatic clear cell renal cell carcinoma

The Ascierto *(36)* anti-PD1 ccRCC cohort was downloaded from GEO (GSE67501). Response data were given as responders or non-responders based on RECIST criteria. The Miao *(37)* anti-PD1 ccRCC data were downloaded from the publication's supplemental information. Responders were classified as patients who either had a complete response (CR) or partial response (PR). This paper consisted of two separate cohorts: a first cohort used for training consisting of fresh tumors and a second cohort used for validation consisting of formalin-fixed paraffin-embedded (FFPE) samples. These two cohorts exhibited different response rates (29.4% vs 18.7%), and transcriptional data indicated sequencing artifacts, so these two cohorts were largely analyzed independently. To merge for survival analysis, RSRD-high patients were determined using optimal thresholds from ROC curves for each cohort and then combined. For the ccRCC anti-PD-L1 IMmotion150 trial*(38)*, data were downloaded from EGA (EGAS00001002928). RNA-seq FASTQ files were quantified to generate TPM using kallisto*(71)* (v0.44.0). Samples with over-expression of genes specific to healthy kidney cells were not used for analysis. Responders were considered as patients with complete or partial response.

Glioblastoma

The Zhao *(41)* GBM anti-PD1 cohort clinical data, including investigator-associated response, were downloaded from the publication's supplemental data. Sequencing data (FASTQ files) were downloaded from SRA (PRJNA482620) and quantified to generate TPM using kallisto*(71)* (v0.44.0). For patients with multiple samples, the latest pretreatment sample was used for analysis. The Cloughesy *(13)* GBM anti-PD1 clinical and transcriptional data were all downloaded from

GEO (GSE121810). This data set consisted of patients treated either in the adjuvant (median survival 417 days) or neoadjuvant (median survival 228.5 days) setting, but did not assess a binary response variable. For survival analysis, a threshold RSRD score was selected as the optimal value from the Zhao cohort ROC curve.

Metastatic prostate cancer

All data from the Subudhi *(53)* cohort of metastatic prostate cancer treated with anti-CTLA4 were acquired from the paper's supplementary materials. This cohort provided overall survival data, and identified 47% of patients as having favorable prognosis following anti-CTLA4 treatment. Based on this, after determining RSRD score from RNA-seq (using TPM), RSRD-high was considered as RSRD scores above the 53rd percentile. The same 53rd percentile threshold was used for TMB, PD-L1 (by IHC), and IMPRES score. Overall survival was assessed using a log-rank test.

Metastatic urothelial cancer

All data for patients with urothelial cancer treated with anti-PD-L1 from Snyder et al. *(43)* were downloaded from http://doi.org/10.5281/zenodo.546110. Response was considered as either PR or CR. Data for the anti-PD-L1 IMvigor210 cohort *(45)* were downloaded from EGA (EGAS00001002556). Based on our previous study *(10)*, a threshold mutation load of 4.46 mutations/Mb was used to classify patients into hypermutated and non-hypermutated groups, selected as the mutation load in TCGA patients that would divide tumors into predominately "M-class" and "C-class" cohorts [as defined in Ciriello et al *(42)*] with maximal separation. For the IMvigor210 cohort, samples collected more than 2 years prior to treatment initiation were excluded, which improved both the predictive ability of neoantigen load in the hypermutated group and the RSRD score in the non-hypermutated group.

Metastatic gastric cancer

Clinical data for metastatic gastric cancer treated with anti-PD-L1*(54)* were retrieved from the publication. RNA-seq data were downloaded from ENA (PRJEB25780) and quantified using kallisto *(71)* (v0.44.0). Responders were considered as patients with complete or partial response. High mutation burden patients were selected as patients with a high mutation load, and low mutation burden patients as patients with a low or moderate mutation load as defined by the authors.

Metastatic melanoma

The Riaz *(55)* anti-PD1 melanoma cohort clinical data were downloaded from the publication's supplemental information, and the RNA-seq data were downloaded from https://www.github.com/riazn/bms038_analysis. The Hugo *(56)* anti-PD1 melanoma cohort clinical data were downloaded from the publication's supplemental information and the RNA-seq data were downloaded from GEO (GSE78220). For both cohorts, responders were considered as patients with complete or partial response. The threshold mutation burden to divide patients into low and high mutation burden groups was selected as the value that resulted in the maximum positive predictive value for mutation burden and maintained at least two responders in the low-mutation cohort. This yielded 87 mutations/Mb in the Riaz cohort and 200 mutations/Mb in the Hugo cohort. In order to have sufficient responders, these two cohorts were merged for analysis of low-mutation patients. Analysis of bulk and high-mutation patients is provided individually.

Alternative biomarker and in silico predicted immune cell populations

The IMPRES*(7)* gene expression score and T Cell Inflamed gene expression signature score *(9, 33)* were calculated as described. For PD-L1 expression, histological scores were used when

available; otherwise, expression of *CD274* (PD-L1) at the gene level was used as a proxy. For cohorts with available data, predictive ability of tumor mutation burden was also analyzed. Immune cell populations in patients were assessed using the xCell *(32)* R package, and pre-calculated TCGA data were directly downloaded from the same website.

TCGA cohorts and analysis

All TCGA data were downloaded using the TCGA data portal (https://portal.gdc.cancer.gov/) from the Pan-Caner Atlas release (April 2018), except for phospho-proteomic data which was acquired from the corresponding manuscript's supplementary information *(51)*. For survival analysis, optimal RSRD threshold values determined from the ICB-treated cohorts were converted to percentiles, and then used to bifurcate patients. For ccRCC, with the exception of multivariate survival analysis, samples were limited to Stage IV patients to best match ICB-treated cohorts. For analysis of urothelial (BLCA) patients, samples were limited to C-class tumors as defined in Ciriello et al *(42)*.

Code availability

kallisto *(71)* (v0.44.0) is available at https://pachterlab.github.io/kallisto/. The xCell*(32)* R package is available at https://github.com/dviraran/xCell or web tool at http://xcell.ucsf.edu/. R packages for survival analysis are available at https://cran.r-project.org/web/packages/survminer/index.html and https://cran.r-project.org/web/packages/survival/index.html. Any additional custom code for analyzing data will be made available upon request.

Supplementary Figures

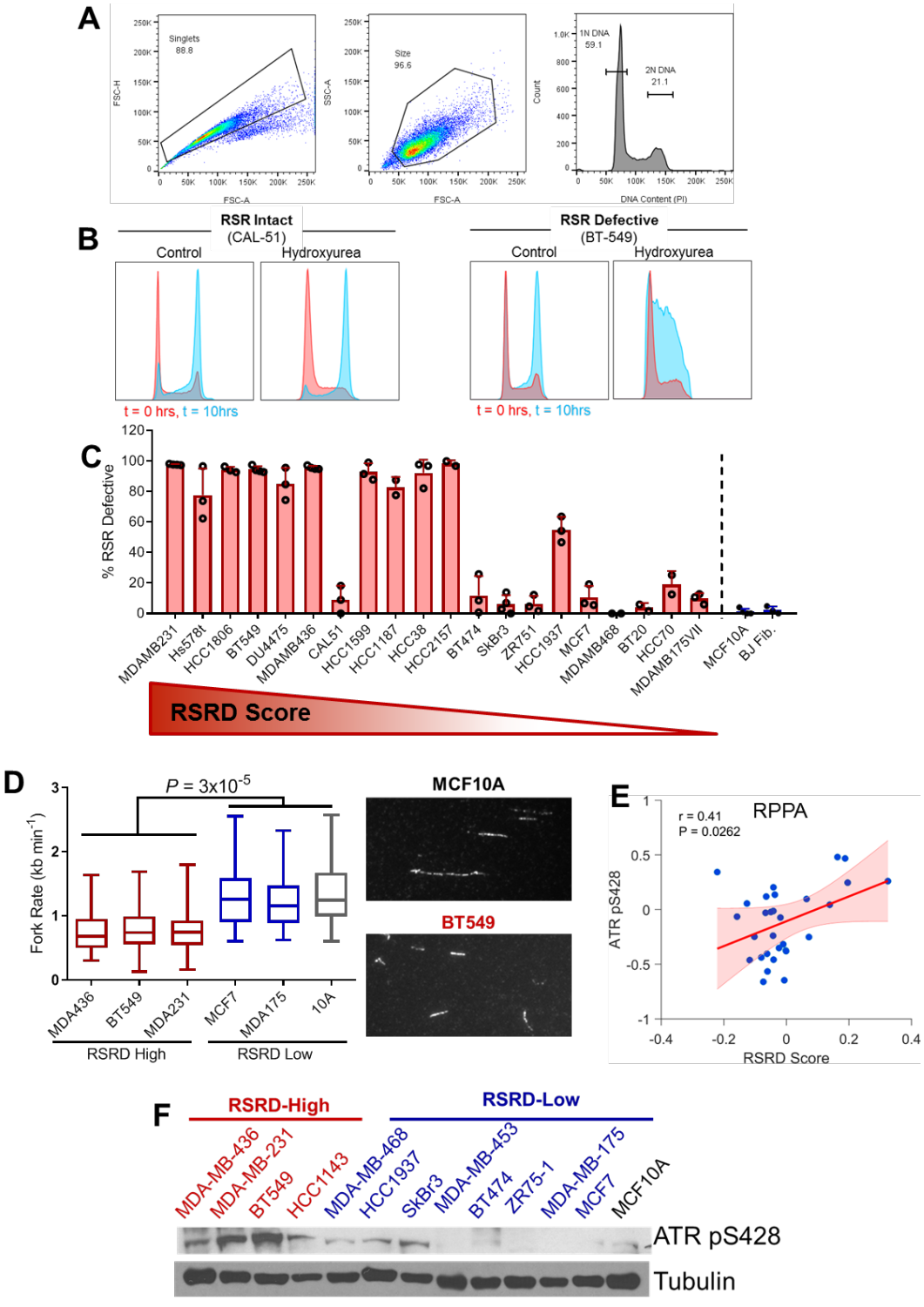

Figure S1. Replication stress response defects in breast cancer.

A, Representative plots showing gating strategy for cell cycle analysis.

B, Representative cell cycle plots for hydroxyurea-induced replication stress recovery cell cycle assay, where RSR function is assessed by fraction of cells capable of completing cell cycle after replication stress *(76)*. Hydroxyurea-induced replication stress synchronizes cells in G1/early S (t = 0 hrs). Cells are released into nocodazole for collection in G2/M for 10 hours (t = 10 hours). Cells with intact RSR will complete the cell cycle, whereas RSR-defective cells will remain in G1/S phase. RSR function is defined from the fraction of cells that reach G2/M after release from HU relative to vehicle-treated cells. RSR-intact CAL-51 cells that can complete S phase in both vehicle-treated and HU-treated conditions, compared to RSR-defective BT-549 cells that fail to complete S phase following hydroxyurea.

C, RSR deficiency as assessed by cell cycle assay across 20 breast cancer cell lines sorted by RSRD score, as well as MCF-10A non-transformed mammary epithelial and BJ fibroblasts. Dots represent biological replicates.

D, Analysis of replication fork speed by DNA fiber assay. Cells were incubated with CldU to label replicating DNA before lysis, and DNA fibers were spread onto glass slides to immunostain individual replication forks. Slower fork speed (shorter DNA fibers) is indicative of higher replication stress.

E, Spearman correlation of RSRD score with ATR phosphorylation as measured by reverse phase protein array (RPPA) *(77)*.

F, Validation of increased ATR phosphorylation in RSRD-high cells by Western blot.

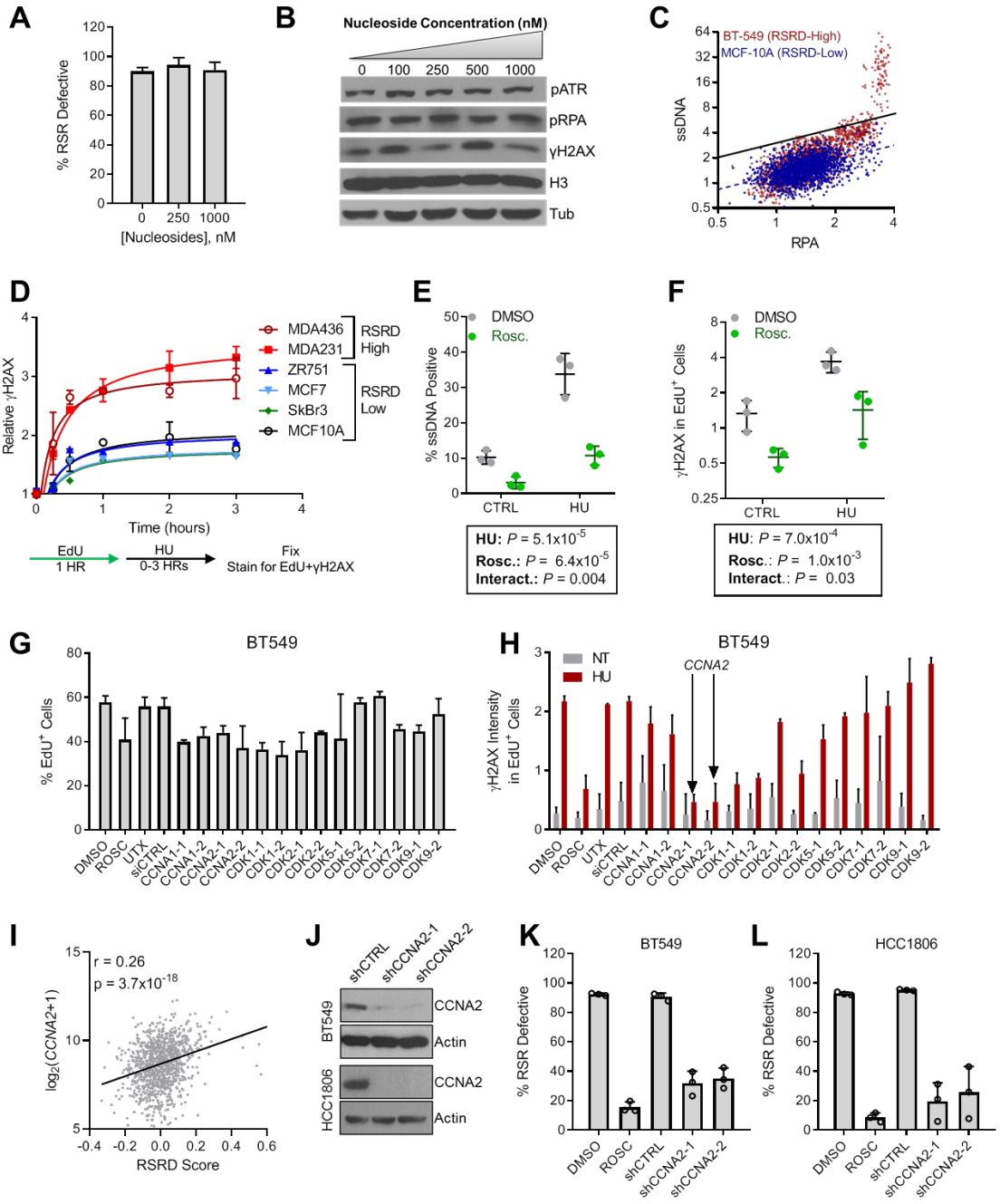

Figure S2. Replication stress response deficiency is caused by aberrant origin firing inducing RPA exhaustion.

A and B, Nucleoside supplementation does not recover RSR-deficient phenotype. Cells were cultured in media supplemented with indicated nucleoside concentrations for 48 hours, replenishing media every 24 hours. (A) RSR defect cell cycle assay per fig. S1A in cells with nucleoside supplementation. Nucleoside supplementation was maintained throughout the course of the assay. (B) Markers of DNA damage and replication stress. Cells were moved to fresh nucleoside-containing media 12 hours before harvesting protein (total nucleoside exposure time = 24 hours + 24 hours + 12 hours = 60 hours).

C, Example graph showing thresholding to identify cells with RPA exhaustion. Dotted line indicates best fit line for vehicle-treated MCF-10A, and solid line contains 99.9% of the MCF-10A cells. RPA-exhausted cells are defined as cells above this threshold, such as vehicle-treated RSRD-high BT-549 cells.

D, Time-dependent formation of double-strand breaks as measured by γH2AX staining following treatment with hydroxyurea. Cells were preincubated with EdU to label S phase cells and then treated with 2 mM HU for indicated times. Intensity of γH2AX was quantified in EdU^+ (S phase) cells and was reported normalized to cells not treated with HU.

E, Suppression of origin firing with roscovitine prevents generation of replication stress as indicated by ssDNA foci. Cells were pretreated with roscovitine for 2 hours or DMSO and then moved to 2 mM HU or vehicle control for 6 additional hours before fixation for immunostaining. Dots represent individual cells; lines mean ± s.d.; inset *P* values determined by two-way ANOVA.

F, Suppression of origin firing prevents replication stress–associated double-strand breaks. Cells were pretreated with roscovitine for 2 hours or DMSO and then moved to 2 mM HU or vehicle control for 6 additional hours before fixation for immunostaining. EdU was added 30 minutes prior to HU for HU-treated cells and 30 minutes prior to fixation for vehicle control cells. Dots represent individual cells; lines mean ± s.d.; inset *P*-values determined by two-way ANOVA.

G and H, Cells were treated with roscovitine (ROSC), vehicle control (DMSO), left untreated (UTX), or transfected with indicated siRNAs before analysis of (G) cycling cells by EdU incorporation or (H) DNA damage in cycling cells as determined by γH2AX.

I, Correlation of *CCNA2* expression with RSRD score in patients with breast cancer from TCGA. Spearman correlation coefficient.

J, Western blot showing stable knockdown of CCNA2 in BT549 cells (top) and HCC1806 cells (bottom).

K and L, RSR function, assessed per Fig. 1A, in either (K) BT549 or (L) HCC1806 cells following treatment of parental lines with roscovitine or DMSO vehicle control, as well as untreated stable cell lines expressing non-targeted control shRNA or shRNAs targeting *CCNA2*.

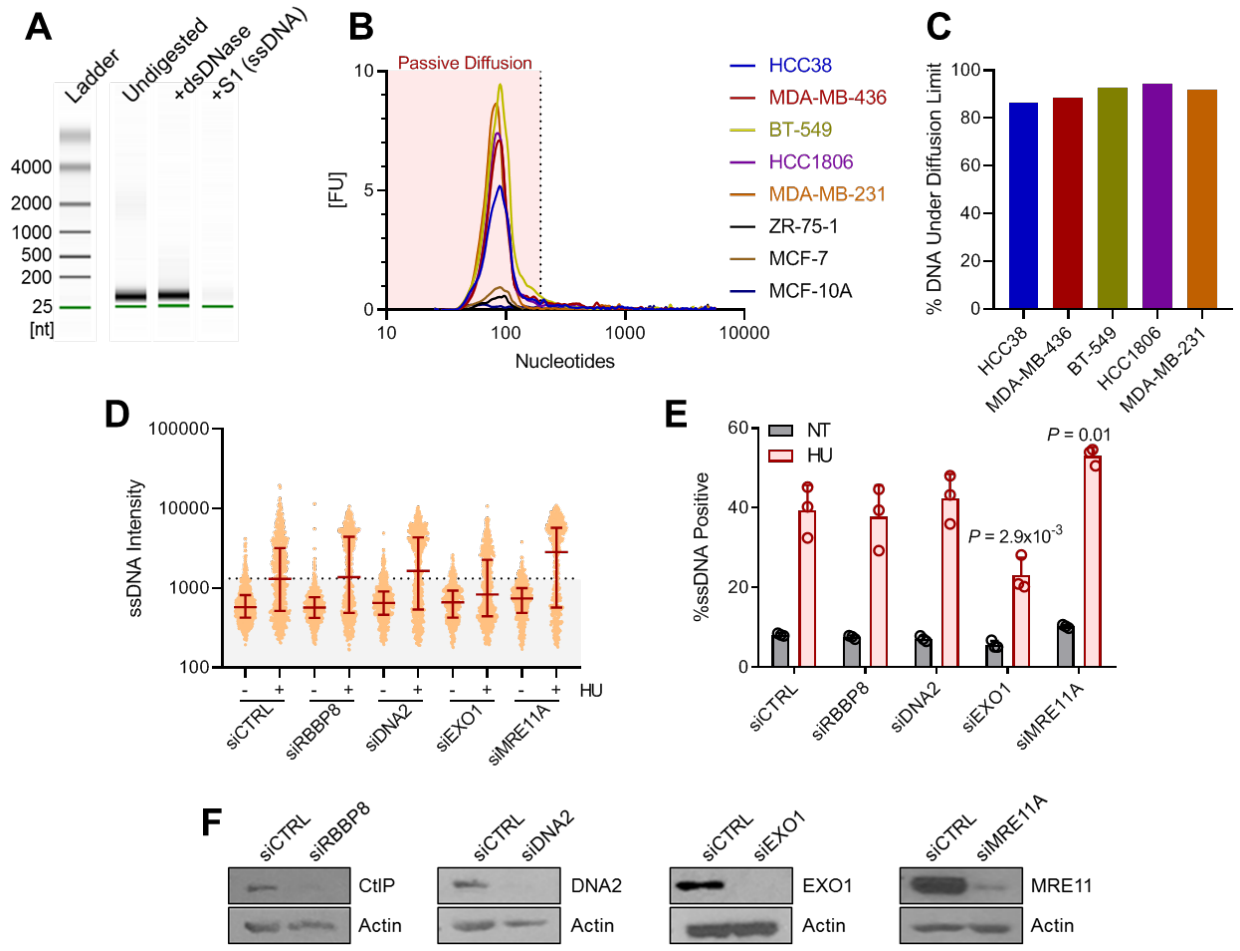

Figure S3. Sources of cytosolic ssDNA.

A, Representative capillary electrophoresis images of cytosolic DNA, as well as following digestion with dsDNase to degrade dsDNA or S1 nuclease to degrade ssDNA.

B, Electrophoregrams of cytosolic DNA extracts for various cell lines. Shaded area indicates size region where DNA can passively diffuse out of the nucleus.

C, Percentage of isolated cytosolic DNA under the diffusion size limit.

D and E, HCC1806 cells were transfected with a pool of two siRNAs targeting the indicated nucleases before staining for ssDNA either before or after treatment with 2 mM HU for 6 hours. Data as shown as (D) ssDNA staining intensity, where shaded region indicates background level, and (E) percentage positive for ssDNA, where each dot represents a biological replicate.

F, Validation of protein knockdown by Western blot.

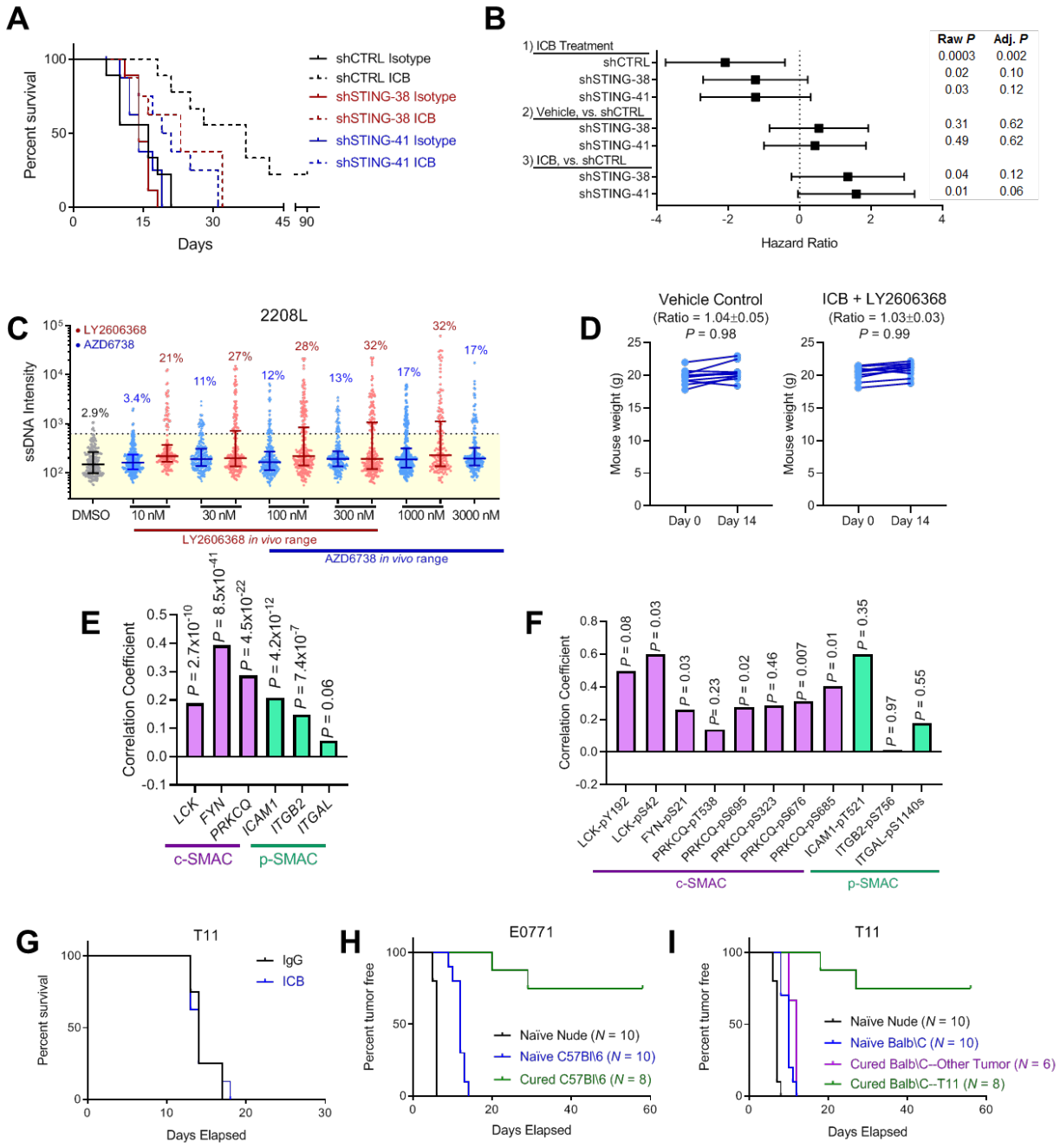

Figure S4. Replication stress response defects in mouse breast cancer models.

A, Survival of mice implanted with RSRD-high T11 cells expressing control shRNA (shCTRL) or shRNA targeting *Tmem173* (shSTING). Mice were treated thrice weekly with ICB consisting of 200 μg anti-PD1 and 100 μg anti-CTLA4. $N = 10$ mice per arm.

B, Log-rank hazard ratios and *P* values for data in (F) comparing: (i) the effect of ICB on survival for each cell line, (ii) survival of STING knockdown lines compared to shCTRL for IgG control-treated arm, and (iii) survival of STING knockdown lines compared to shCTRL in the ICB-treated arm. Raw and Holm-corrected adjusted *P* values shown.

C, Washout assay following 12-hour treatment with 100 nM LY2606368 or DMSO vehicle control in RSRD-low 2208L cells. Each dot represents an individual cell.

D, Bodyweights of mice bearing 2208L tumors either given control treatments (control IgG and vehicle solvent) or combination of CHK inhibitor LY2606368 and ICB consisting of 200 μg anti-PD1 and 100 μg anti-CTLA4 prior to start of treatment (Day 0) and either at Day 14 or point of euthanasia due to tumor burden, whichever came first. Inset ratio is mean ± std of the ratio of weight at Day 14 to Day 0, indicating slight weight gain in both groups. *P* value determined by right-tailed paired *t*-test, that is probability that mouse weights decreased upon treatment.

E, Spearman correlation coefficient between RSRD score and gene expression levels of specified immunological synapse components in TCGA breast cancer patients.

F, Spearman correlation coefficient between RSRD score and phospho-protein levels of specified immunological synapse components in TCGA breast cancer patients.

G, Kaplan Meier plots for mice bearing the ICB-sensitive/RSRD-high T11 model in nude mice lacking T cells following treated with ICB as described in Fig. 3, E to I.

H, Kaplan Meier plots for tumor formation rate following implantation of RSRD-high E0771 into either naïve nude mice, naïve C57Bl/6 mice, or C57Bl/6 mice previously implanted with E0771 cells 6 months after achieving a complete response to ICB.

I, As described in (H), except using RSRD-high T11 cells. An additional control of Balb/C previously cured using ICB in an unrelated tumor model is also included.

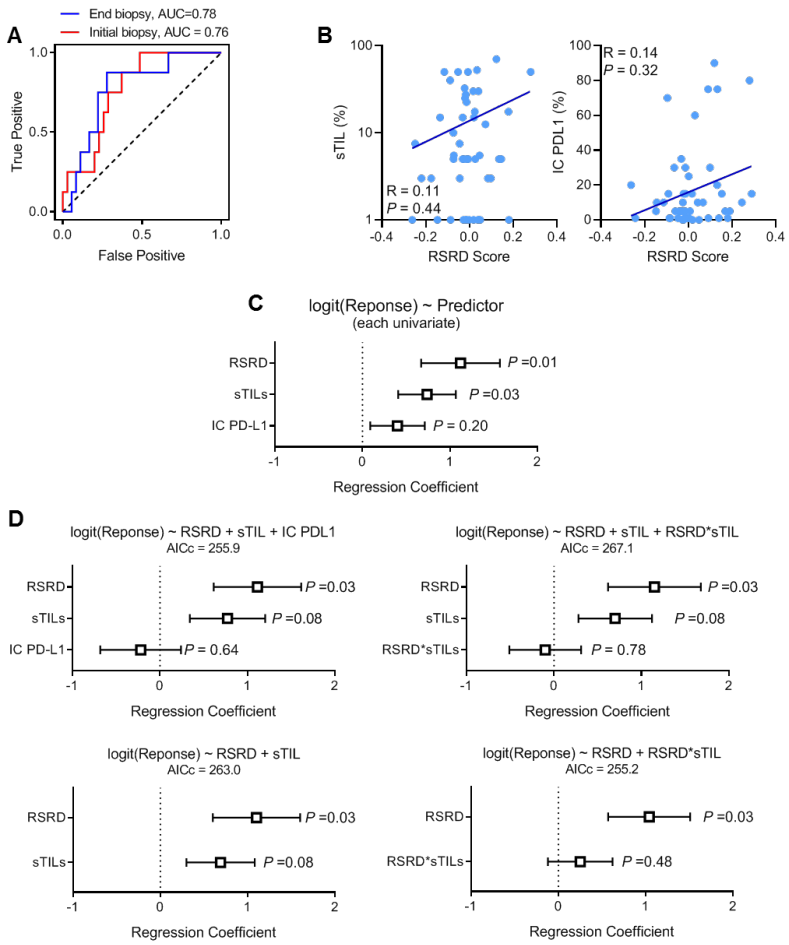

Figure S5. RSRD score is an independent biomarker of ICB response in the TONIC breast cancer cohort.

A, ROC plots showing prediction of ICB response by RSRD score in TONIC cohort using either end-point biopsies or initial biopsies.

B, Correlation between RSRD score and sTILs or PDL1 on immune cells (IC PDL1). Spearman rank correlation.

C, Univariate logistic regression coefficients for the three biomarkers to predict response to ICB, defined as SD/PR/CR.

D, Multivariate logistic regression to predict ICB response using various models as indicated. AICc indicates Akaike information criterion for small samples, where smaller values generally indicate a better model.

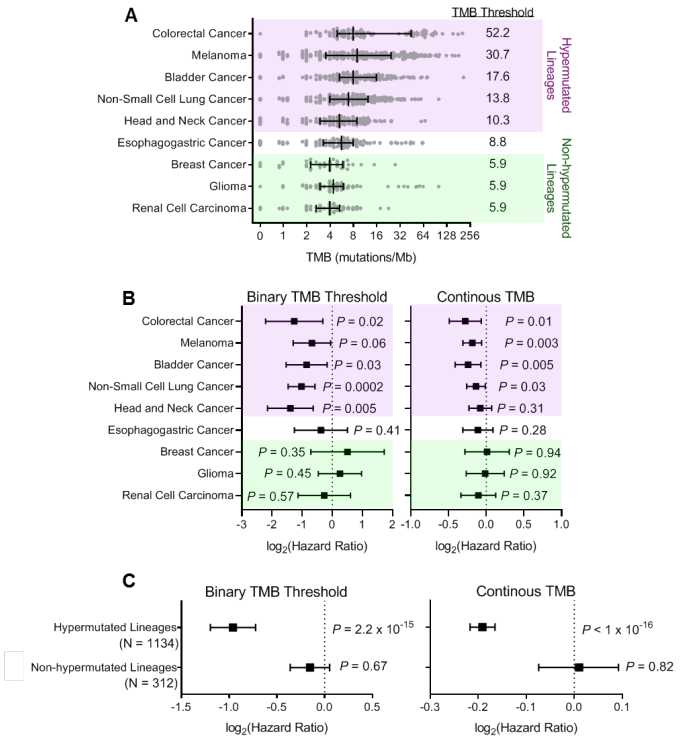

Figure S6. Tumor mutation burden (TMB) does not predict response to ICB in non-hypermutated lineages.

A, Distribution of TMB values for cohorts from Samstein et al *(3)* and division into hypermutated and non-hypermutated tumor lineages. Inset values show threshold values for high vs low TMB tumors within each tumor lineage used in Samstein et al. Tumors of unknown origin are excluded.

B, Hazard ratios for patients treated with immune checkpoint blockade determined by log-rank test for the binary TMB, and Cox proportional hazards model for continuous TMB. For the binary model, thresholds from S6A were used. For the continuous model, TMB values were transformed by $\log_2$(TMB+0.1).

C, Hazard ratio for patients treated with immune checkpoint blockade determined by Cox proportional hazards model pooling either patients with hypermutated cancers or patients with non-hypermutated cancers, with tumor lineage used as a clustering variable. For the binary model, thresholds from S6A were used. For the continuous model, TMB values were transformed by $\log_2$(TMB+0.1).

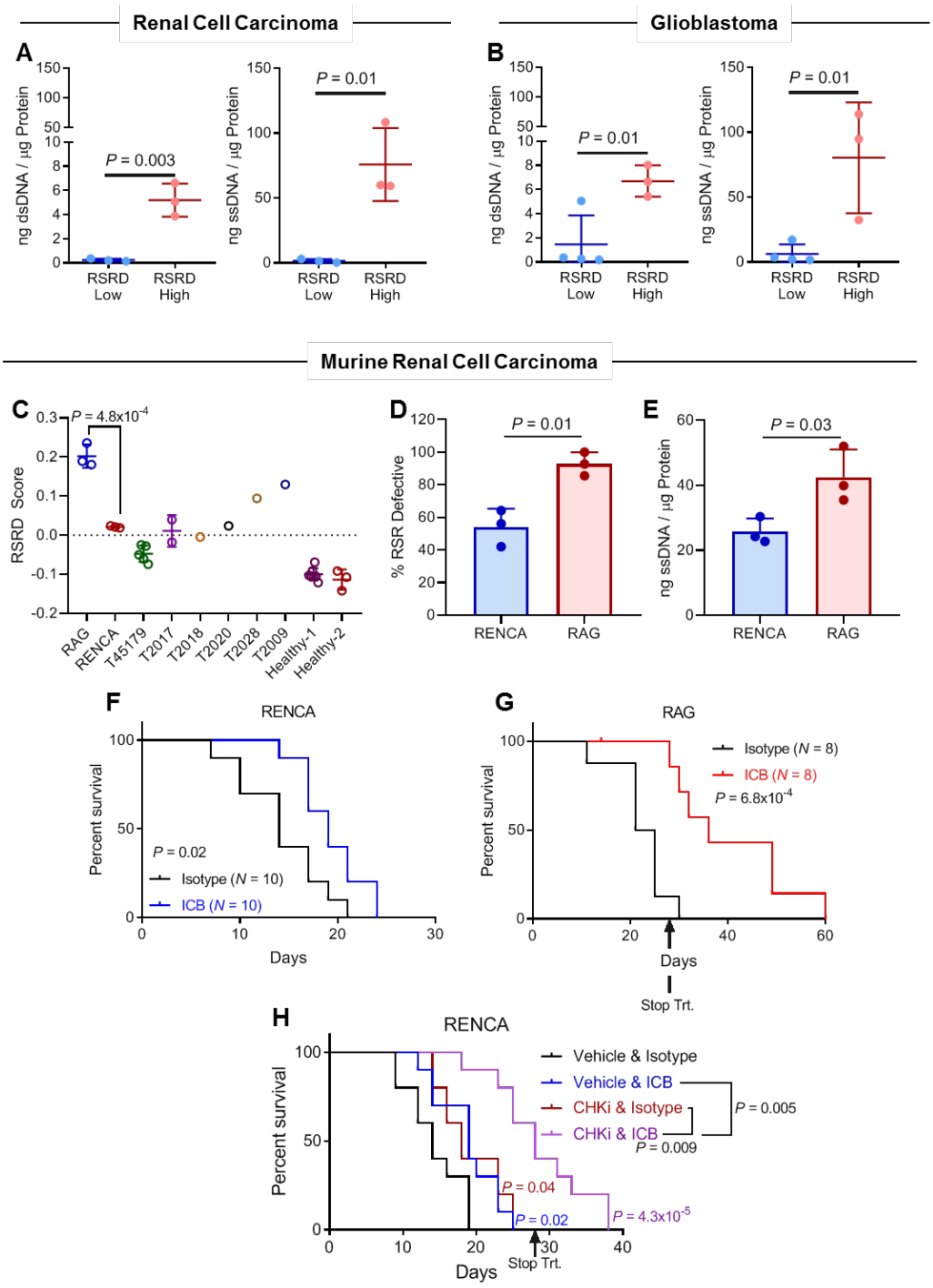

Figure S7. Applicability of RSRD score in other cancer types.

A and B, Cytosolic fractions were isolated and used for quantification of cytosolic DNA normalized to cytosolic protein concentration in RSRD-high and RSRD-low ccRCC cell lines (A) and GBM cell lines (B). Dots indicate individual cell lines; lines mean ± s.d.; *P* value determined by *t* test.

C, RSRD score in RAG and RENCA cells, as well as tumors derived from a mouse with renal-specific deletion of *Vhl* and *Pbrm1* (T45179) *(36)*, tumors derived from multiple mice with renal-

specific deletion of *Vhl*, *Trp53*, and *Rb1* (T2017, T2018, T2020, T2028, T2009) *(37),* healthy controls paired with the *Pbrm1*/*Vhl* tumors (Healthy-1), or healthy controls paired with the *Vhl*/*Trp53*/*Rb1* tumors (Healthy-2).

D, Quantification of RSRD function in RENCA and RAG cells by cell cycle restart assay as described in Fig. 1A.

E, Quantification of cytosolic ssDNA in RENCA and RAG cells as described in Fig. 2J.

F and G, Kaplan Meier plots for selected moderately RSRD (F, RENCA) and RSRD-high (G, RAG) murine in vivo models following treatment with ICB (10 mg/kg anti-PD1, thrice weekly) compared to isotype control. Significance determined by log-rank test.

H, Kaplan-Meier plots for RENCA tumors treated with either vehicle control, ICB, CHK1i (prexasertib/LY2606368), or combination of ICB and CHK1i. Treatment was ceased after 4 weeks. $N = 10$ mice per group. Significance determined by log-rank test.

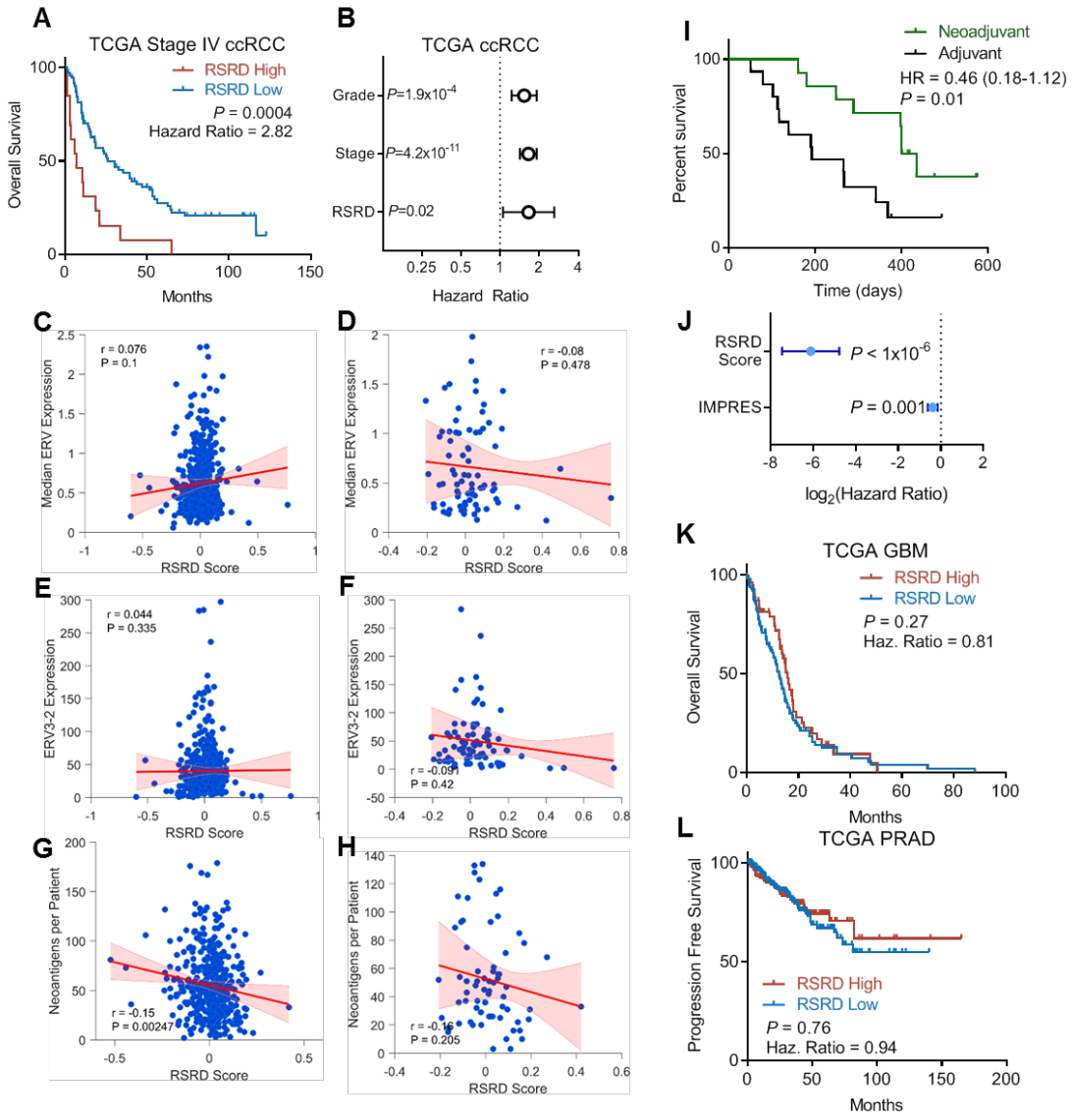

Figure S8. RSRD score in patients from TCGA not treated with ICB.

A and B, RSRD score is a negative prognosticator in ccRCC not treated with ICB. (A) Stage IV ccRCC patients from TCGA were split into RSRD-high and RSRD-low patients based on the optimal percentile determined from AUC plots for the Miao cohorts in Figure 6A. Significance determined by log-rank test. (B) Multivariate analysis using Cox proportional hazards model considering RSRD score, tumor grade, and tumor stage for all ccRCC patients in TCGA.

C, RSRD score is more highly expressed in ccRCC, which responds to ICB, compared to chromophobe RCC, which has minimal response to ICB. Log-rank *P* value.

C to F, Correlation between RSRD score and exogenous retrovirus expression *(38)* in either all patients (C and E) or Stage IV only (D and F), quantified either as median expression of all ERVs (C and D), or expression of ERV3-2 (E and F). Spearman correlation coefficient.

G and H, Correlation between RSRD score and neoantigen load in either all patients (G) or Stage IV only (H). Spearman correlation coefficient.

I, Overall survival stratified by treatment in neoadjuvant or adjuvant setting.

J, Multivariate analysis of RSRD score and IMPRES score by Cox proportional hazards model using neoadjuvant/adjuvant as a clustering variable.

K, RSRD score is prognostically neutral in GBM. GBM patients from TCGA were split into RSRD-high and RSRD-low patients based on the optimal percentile determined from AUC plots for the Zhao cohort in Fig. 6D. Significance determined by log-rank test.

L, RSRD score is prognostically neutral in prostate cancer. PRAD patients from TCGA were split into RSRD-high and RSRD-low patients at 55^{th} percentile to correspond with value in Fig. 7, H and I. Significance determined by log-rank test.

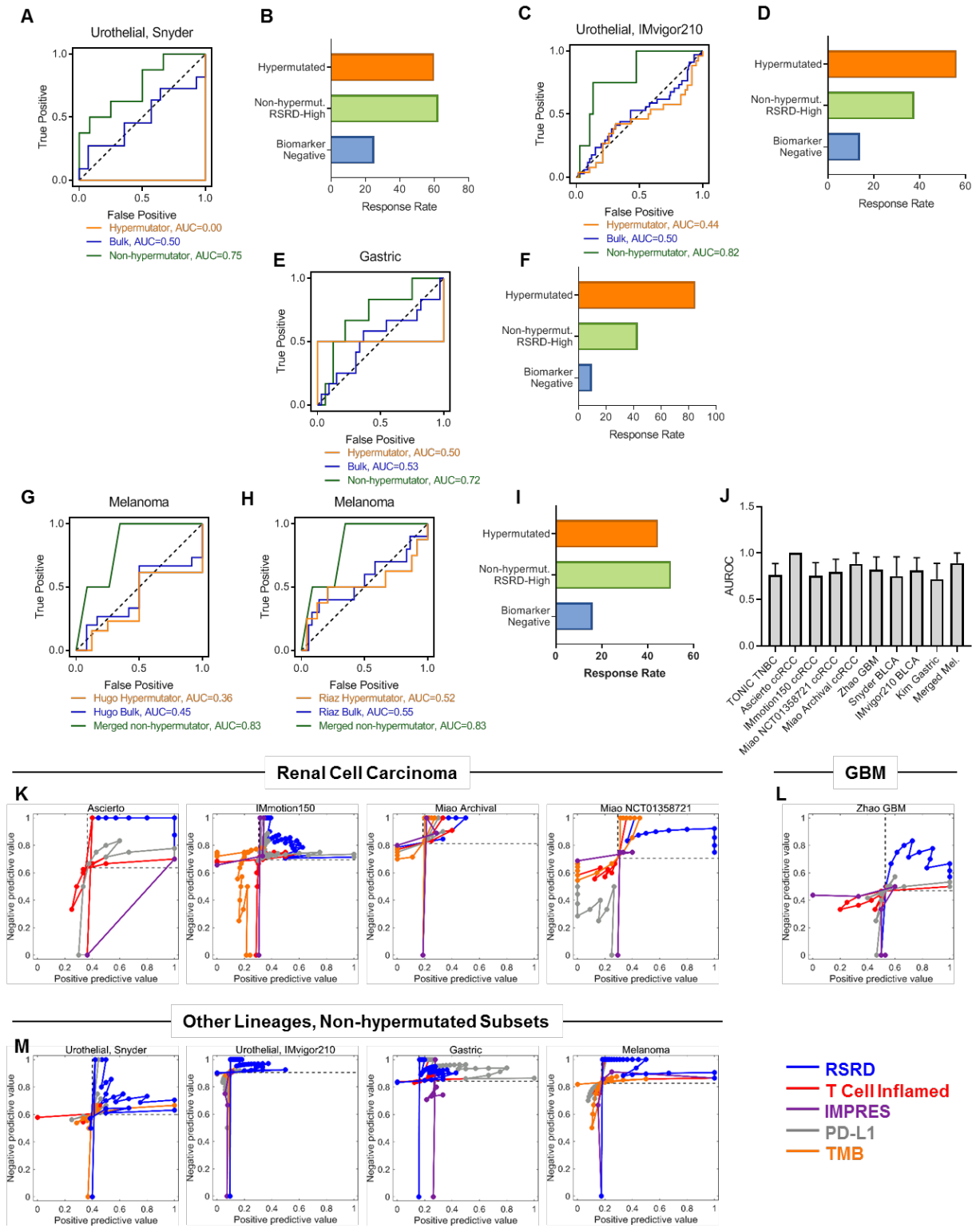

Figure S9. Prediction of ICB response by RSRD score in patients stratified by mutation burden.

A, ROC curves for the ability of RSRD score to predict ICB response in patients with urothelial cancer treated with anti-PD-L1 from Snyder et al *(42)* within the hypermutated cohort, non-hypermutated cohort, or non-stratified bulk cohort.

B, Response rates for patients with urothelial cancer in (A) that are hypermutated, low-mutation and RSRD-high, or negative for both biomarkers.

C, ROC curves for the ability of RSRD score to predict ICB response in patients with urothelial cancer treated with anti-PD-L1 from IMvigor210 *(44)* within the hypermutated cohort, non-hypermutated cohort, or non-stratified bulk cohort.

D, Response rates for patients with urothelial cancer in (C) that are hypermutated, non-hypermutated and RSRD-high, or negative for both biomarkers.

E, ROC curves for the ability of RSRD score to predict ICB response for patients with gastric cancer treated with anti-PD-L1*(71)* within the hypermutated cohort, non-hypermutated cohort, or non-stratified bulk cohort.

F, Response rates for patients with urothelial cancer in (E) that are hypermutated, non-hypermutated and RSRD-high, or negative for both biomarkers.

G and H, ROC curves for the ability of RSRD score to predict ICB response in melanoma patients within the hypermutated cohort, non-hypermutated cohort, or non-stratified bulk cohort. For sufficient sample size, the patients with non-hypermutated tumors were pooled between the Hugo and Riaz cohorts treated with anti-PD1 *(72, 73)*. Prediction is shown for hypermutated and non-stratified bulk populations individually for the Hugo (E) and Riaz (F) cohorts compared to the merged non-hypermutated cohort.

I, Response rates for melanoma cancer patients (G and H) that are hypermutated, non-hypermutated and RSRD-high, or negative for both biomarkers.

J, Boot-strapped 95% confidence intervals for area under ROC curves (AUROC) for all patient cohorts with objective response data.

K to M, Relationship between positive predictive value and negative predictive value across all threshold values for (K) renal cell carcinoma, (L) glioblastoma, and (M) non-hypermutated subsets of other cancer lineages.

Table S1. Cell lines, sources, and media formulations.

Table S2. Antibodies used in this study.

Table S3. siRNA and shRNA used in this study.

Table S4. Raw RNA-seq of murine RCC cell lines

Data file S1. Raw data for figures